PT-Symmetry-Enabled Spin Circular Photogalvanic Effect in Antiferromagnetic Insulators

Ruixiang Fei,[1,*] Wenshen Song,[1] Lauren Pusey-Nazzaro,[1] and Li Yang[1,2,†]
[1]*Department of Physics, Washington University in St. Louis, St. Louis, Missouri 63130, USA*
[2]*Institute of Materials Science and Engineering, Washington University in St. Louis, St. Louis, Missouri 63130, USA*

(Received 10 April 2021; revised 30 July 2021; accepted 20 October 2021; published 12 November 2021)

The short timescale spin dynamics in antiferromagnets is an attractive feature from the standpoint of ultrafast spintronics. Yet generating highly polarized spin current at room temperature remains a fundamental challenge for antiferromagnets. We propose a spin circular photogalvanic effect (spin CPGE), in which circularly polarized light can produce a highly spin-polarized current at room temperature, through an "injection-current-like" mechanism in parity-time (*PT*)-symmetric antiferromagnetic (AFM) insulators. We demonstrate this effect by first-principles simulations of bilayer CrI_3 and room-temperature-AFM hematite. The spin CPGE is significant, and the magnitude of spin photocurrent is comparable with the widely observed charge photocurrent in ferroelectric materials. Interestingly, this spin photocurrent is not sensitive to spin-orbit interactions, which were regarded as fundamental mechanisms for generating spin current. Given the fast response of light-matter interactions, large energy scale, and insensitivity to spin-orbit interactions, our work gives hope to realizing fast-dynamic and temperature-robust pure spin current in a wide range of *PT*-symmetric AFM materials, including topological axion insulators and weak-relativistic magnetic insulators.

DOI: 10.1103/PhysRevLett.127.207402

Introduction.—Spintronics based on antiferromagnetic (AFM) materials has great potential in reducing device scale and power consumption [1–3]. In contrast to ferromagnets, AFMs are robust against perturbed magnetic fields, produce no stray fields, and are capable of generating large magnetotransport effects [1], making them promising for next-generation spintronics. Particularly, AFMs exhibit unique advantages in generating spin current, which is the basis for spintronic devices. Compared with gigahertz microwave pulses used in ferromagnets, terahertz pulses can pump spin current by exciting the left- and right-hand modes of magnons in AFMs [4–6] due to strong exchange interactions, giving rise to ultrafast spin dynamics [7]. Additionally, spin caloritronics based on magnons in AFMs, such as spin Seebeck and spin Nernst effects [8–11], was proposed to generate pure spin current in the same device. However, because of the intrinsically small energy scales, magnon-based spin current decays rapidly with increasing temperature [5,12], making it difficult for room-temperature device applications.

Optical pump-induced spin dynamics may be a promising approach to surmounting such difficulties because of its intrinsically larger energy scale [13,14] and observed strong light-matter interactions in magnetic materials [15–17]. Notably, second-order light-matter interactions, such as the circular photogalvanic effect (CPGE) or bulk photovoltaic effect (BPVE), are known to create charge current in polar materials at room temperature without bias [18–23]. Recently, this idea has been extended to two-dimensional (2D) parity-time (*PT*) symmetric AFM insulators [24] and topological axion insulators [25,26], in which a sizable dc charge current was predicted to be generated by linearly polarized light [24,25,27].

Beyond charge current, light can also drive spin current [28–35]. For example, spin photocurrent was predicted in AFM hematite [31] and bilayer $CrCl_3$ [36] via the shift-current mechanism under linearly polarized light, denoted as the spin-BPVE [31]. Unfortunately, linearly polarized light simultaneously excites significant charge current because of the broken SU(2) symmetry due to spin-orbit coupling (SOC) [24,25], substantially diluting spin polarization of the overall current. Consequently, it remains a fundamental challenge to generate highly polarized spin current in AFMs at room temperature.

In this work, we predict a spin circular photogalvanic effect (spin CPGE), in which circularly polarized light can generate pure spin current in *PT*-symmetric antiferromagnets. This effect arises from a second-order light-matter interaction, i.e., an inject-current-like mechanism. We demonstrate this prediction by first-principles simulations of two typical *PT*-symmetric antiferromagnets: low-temperature-AFM bilayer CrI_3 and room-temperature-AFM three-dimensional (3D) hematite. Because of *PT* symmetry and circular polarization, charge current is induced by the shift-current mechanism while pure spin current is induced by the inject-current-like mechanism. Importantly, the magnitude of spin current is about 1 to 2 orders larger than that of charge current, resulting in highly spin-polarized photocurrent.

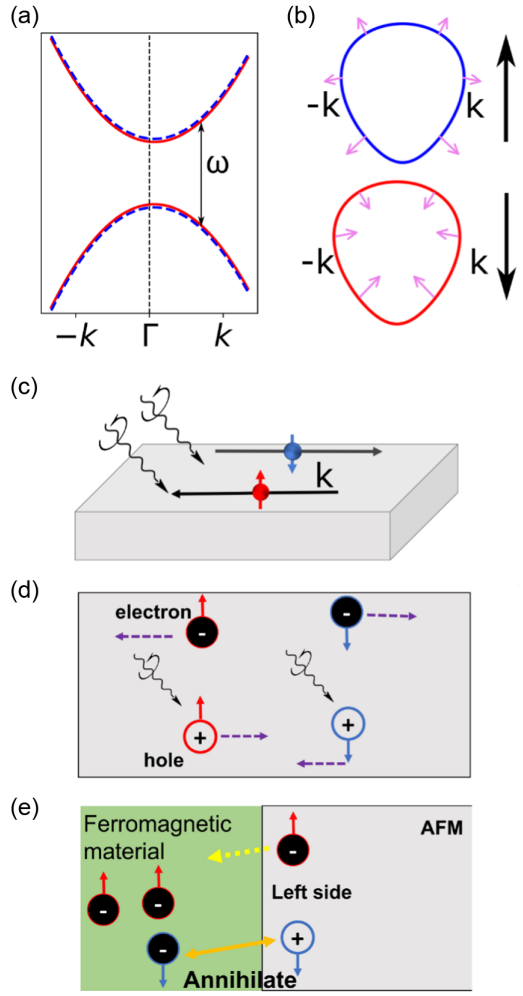

FIG. 1. (a) Doubly degenerate bands due to PT symmetry. (b) The transport direction of the two opposite directions of spins due to PT symmetry after pumping. The blue and red ovals represent the contour plot of the two spin components' conduction bands, and the black arrows show the overall spin-current direction. (c) The schematic of circularly polarized light-induced spin current under circularly polarized light. (d) The circularly polarized light generated electron and hole travel in opposite directions. Here, we define the light generated spin-down electron and -down hole pair. Solid and open circles represent electrons and holes, respectively. The arrows of the circles represent spin directions. (e) The proposed experimental setup. The spin-down hole will annihilate with a spin-down electron after being injected into the FM material.

Moreover, we unexpectedly find that SOC is nonessential for generating a spin photocurrent. Our work suggests that collinear PT-symmetric AFMs, even weak-relativistic examples, can serve as effective and temperature-robust spin generators via ultrafast light-matter interactions.

PT-symmetry induced chiral spin photocurrent.—Let us consider an AFM insulator that breaks both time-reversal symmetry (T) and parity symmetry (P) but respects PT. The Hamiltonian satisfies $H(k,\uparrow) = H(k,\downarrow)$ for any k wave vector, resulting in exactly double spin-degenerate bands, as shown in Fig. 1(a). Because of these degenerate bands and zero Abelian Berry curvature, a bias field cannot effectively drive the longitudinal or transverse spin current in PT-symmetric AFM insulators. Nevertheless, after involving second-order light-electron interactions for the nonbiased case, these degenerate spins exhibit different behaviors, enabling a spin-polarized photocurrent.

For a coherent light illumination, the general form of a second-order dc photocurrent is $J_c = \chi_{abc}(0;\omega,-\omega) \times E_a(\omega)E_b(-\omega)$, where $\chi_{abc}(0;\omega,-\omega)$ is the dc photoconductivity. For light circularly polarized in the ab plane, the inject-current-like spin photoconductivity $\eta^{\circlearrowleft,\alpha}_{abc} \equiv \chi_{abc}(0;\omega,-\omega)$ under the relaxation-time approximation is [19,37]

$$\eta^{\circlearrowleft,\alpha}_{abc} = \frac{-\pi e^3}{\hbar^2\omega^2}\sum_{mn}\int d^3k \mathrm{Im}[v^a_{mn,\alpha}(k)v^b_{nm,\alpha}(k)] \times f_{mn}(\langle m|\{\sigma_\alpha, v_c\}|m\rangle\tau_m - \langle n|\{\sigma_\alpha, v_c\}|n\rangle\tau_n)\delta(\omega-\omega_{mn}), \quad (1)$$

where $\mathrm{Im}[v^a_{mn,\alpha}(k)v^b_{nm,\alpha}(k)] = \frac{1}{2}[v^a_{mn,\alpha}v^b_{nm,\alpha}(k) - v^b_{mn,\alpha}(k) \times v^a_{nm,\alpha}(k)]$ is the imaginary part of optical oscillator strength. $v^a_{mn,\alpha}(k)$ and $v^b_{nm,\alpha}(k)$ are the a-direction and b-direction interband velocity matrix elements between the mth and nth bands with α spin, respectively. $f_{mn} = f(\epsilon_{mk}) - f(\epsilon_{nk})$ is the occupation number difference. τ_m is the minimum value of spin-relaxation and free-carrier relaxation times of the mth band carrier. $\{\sigma_\alpha, v_c\} = \frac{1}{2}(v_c\sigma_\alpha + \sigma_\alpha v_c)$ and $\langle m|\{\sigma_\alpha, v_c\}|m\rangle$ is the c-direction velocity matrix of the mth band carrier with α-direction spin. The optical selection rules of circularly polarized light should be satisfied by the orbital angular momentum of involved electronic states. It is worth noting that spin current may not be well defined for systems with strong SOC. However, Shi *et al.* proved that the traditional definition of spin current remains a good approximation if the spin-relaxation time is long or SOC is weak [38]; our following predictions are for materials fitting these criteria.

From PT symmetry, electronic bands are spin degenerate, and the group velocity matrix of two spins should be in the same direction, namely, the spin velocity matrices satisfy $\{\sigma_\uparrow, v_c\} = \{\sigma_\downarrow, v_c\}$. However, the PT symmetry enforces a constraint: $\mathrm{Im}[v^a_{mn,\uparrow}(k)v^b_{nm,\uparrow}(k)] = -\mathrm{Im}[v^a_{mn,\downarrow}(k)v^b_{nm,\downarrow}(k)]$. Therefore, the spin-"up" photoconductivity of Eq. (1) is opposite to the spin-"down" photoconductivity. Since the overall spin photoconductivity is defined as $\eta^s = \eta(\uparrow) - \eta(\downarrow)$, we expect a pure spin-current contribution. Finally, the overall spin current is obtained by an integral over the whole reciprocal space. As shown in Fig. 1(b), if the energy contour of light-pumped free carriers is not symmetric, which is the typical case in noncentrosymmetric materials, the integral spin current is nonzero. Intuitively, the light-driven electron

transportations are helical channels where the electron spin projection is connected with its transport direction: the spin-up electrons are traveling in one direction, while the spin-down electrons are moving in the opposite direction, generating a pure spin current shown in Fig. 1(c).

Light will create electrons and holes simultaneously, and the total spin-current is composed of the hole and electron contributions in Eq. (1). Figures 1(e) and 1(e) illustrate the roles of electrons and holes and how to measure spin current. We define the light-generated spin-down electron and spin-down hole pair (or spin-up electron and spin-up hole pair) as shown in Fig. 1(d). Under circularly polarized light, the excited holes and electrons with the same spin direction should travel in opposite directions. In Fig. 1(e), the spin-up electrons and spin-down holes are accumulated at the left boundary of the AFM insulator. If attached to a FM material, in which the majority is assumed to be spin-up, the spin-down holes will annihilate with the minority spin-down electrons in the FM material while the spin-up electrons remain. As an example, the magnetic momentum of the attached FM part is increased from $+1\ \mu_B$ to $+3\ \mu_B$, resulting in a measured spin-polarized current contributed from both electrons and holes.

In addition to the injection-current mechanism, shift current can be simultaneously excited by circularly polarized light, which will affect the spin polarization. The shift-current photoconductivity under circularly polarized light is

$$\sigma^{\circlearrowleft}_{abc}(0;\omega_{in},-\omega_{in}) = \frac{-\pi e^3}{\hbar^2\omega^2}\sum_{m,n}\int\frac{d^3k}{(2\pi)^3}(\langle m|v_a|n\rangle\langle n|v_b|m\rangle_{;c} - \langle m|v_b|n\rangle\langle n|v_a|m\rangle_{;c})\delta(\omega-\omega_{mn}), \tag{2}$$

where $\langle n|v_b|m\rangle_{;c} = (\partial\langle n|v_b|m\rangle/\partial k^c) - i(A^c_{nn} - A^c_{mm})$ are the "generalized derivatives" of the velocity matrix element and A^c is the intraband Berry connection along the c direction. Unlike linearly polarized light [31], shift current is PT even, contributing to charge current. Fortunately, because the magnitude of shift current is usually 2 orders smaller than that of injection current [24,25,39], the overall observed photocurrent is dominated by injection current and, thus, highly spin polarized, which is confirmed by the following *ab initio* simulations.

Large photodriven spin current in two-dimensional materials.—We employ first-principles simulations (see Supplemental Material [40]) [41–43] to calculate spin photocurrent of PT-symmetric bilayer AFM CrI_3. Its bulk structure belongs to the S_6 point group which possesses an out-of-plane C_3 axis and lacks a mirror plane. The top view is illustrated by Fig. 2(a), and the blue and red atoms represent the spin-up-layer and spin-down-layer Cr atoms, respectively. Our first-principles calculations indicate that bilayer CrI_3 has an interlayer AFM ground state, in agreement with previous results [17,44,45]. The doubly

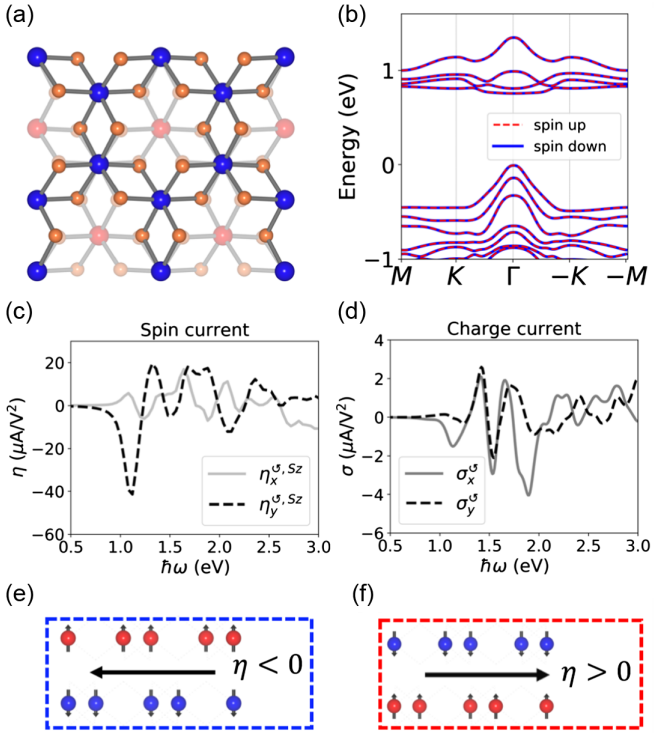

FIG. 2. The atomic structure (a) and band structure (b) of bilayer AFM CrI_3. (c) The photodriven spin-current conductivity along the in-plane x and y direction for spin S_z. (d) The photodriven charge-current conductivity along the x and y direction. (e) and (f) The spin-current direction for AFM bilayer CrI_3 (side view of Cr atoms) with opposite Néel vector directions.

degenerate bands in momentum space due to PT symmetry are shown in Fig. 2(b).

Figure 2(c) shows the spin photoconductivity according to Eq. (1). We set the circular polarization of light to be in the xy plane and measure the S_z spin current. Because of the depolarization efect and 2D geometry, there are two nonzero components, which are $\eta^{\circlearrowleft,Sz}_x$ (along the x direction) and $\eta^{\circlearrowleft,Sz}_y$ (along the y direction), respectively. There is no widely accepted carrier lifetime τ [Eq. (1)] of CrI_3. Previous works [24] adopted ~0.4 ps, which is smaller than those of transition metal dichalcogenides, such as MoS_2 (~1 ps) [46]. Here, we choose a more conservative value of 0.1 ps in Eq. (1), and it is orders smaller than the spin-relaxation time of typical 2D materials (approximate nanoseconds) [47].

The spin photoconductivity is significant, e.g., the $\eta^{\circlearrowleft,Sz}_y$ can reach up to 40 $\mu A/V^2$ shown in Fig. 2(c). This is roughly one order of magnitude larger than the widely observed charge photoconductivity of $BaTiO_3$ [48], 2D GeS and its analogs [49] due to BPVE. Moreover, the magnitude of this spin current is comparable with those of spin-polarized photocurrents in nonmagnetic CdSe and GaAs quantum wells [50–52].

In addition to spin current from the inject current mechanism, circularly polarized light can simultaneously

generate a charge current via the shift-current mechanism [Eq. (2)]. Figure 2(d) shows the charge-current photoconductivity for circularly xy plane-polarized light. Similar to spin photocurrent, the two nonzero tensors $\sigma_x^{\circlearrowleft}$ and $\sigma_y^{\circlearrowleft}$ are not equivalent due to the C_3 rotation symmetry. Comparing Figs. 2(c) and 2(d), the charge current is around 1-to-2 orders of magnitude smaller than the spin current, resulting in a more than 90% spin polarization.

Finally, we predict that the direction of spin photocurrent can be switched by the Néel vector. Although both configurations in Figs. 2(e) and 2(f) are AFM, their spin currents are opposite to each other. This is because the magnetic structure indicated in the blue dashed square can be translated to that in the red dashed square by the space-reversal operator (P). Accordingly, the direction of current is switched by P. This correlation between the Néel vector and spin photocurrent is useful for detecting the Néel vector, which has been regarded as a challenge for years [53].

Sizable photodriven spin current without SOC.—SOC is viewed as one of the foundations for spin current because it can generate spin-polarized currents from charge current, characterized as the spin Hall effect [54–56]. Besides, SOC lies at the heart of the photodriven charge current in PT-symmetric AFMs, e.g., bilayer CrI_3 [24] and even-septuple layer $MnBi_2Te_4$ [25], breaking the SU(2) symmetry. Therefore, it is necessary to reveal the origin of such an enhanced spin photocurrent and the role of SOC.

We have calculated the spin photoconductivity η of bilayer AFM CrI_3 by gradually reducing the SOC strength (λ_{so}). We take the y-direction spin photocurrent as an example (see x direction in Supplemental Material [40]), and the results are presented in Fig. 3(a): the solid line is the spin photoconductivity with intrinsic SOC strength, and the dashed line is that with negligible SOC ($\lambda = 0.001\lambda_{so}$). The band structures are provided in the Supplemental Material [40]. Despite different band structures due to SOC, the magnitudes of two spectra are similar; the spin photoconductivity of the dashed line can reach 45 $\mu A/V^2$, which is slightly larger than that with full SOC. This surprisingly indicates that SOC is not necessarily responsible for enhanced spin photocurrents.

To further understand this result, we show the spin texture of the valence band $E = -0.17$ eV (zero energy is at the top of valence bands) with full SOC for bilayer CrI_3 in Fig. 3(b). Importantly, the bands are not symmetrical, e.g., the oval-shaped energy contour of the inner band, a consequence of broken SU(2) spin-rotation symmetry by SOC. Therefore, the spin photoconductivity at the k point cannot cancel with that at the $-k$ point. We illustrate this by plotting the distribution of spin photoconductivity in k space in Fig. 3(c). There is a non-odd-parity symmetry of this distribution, which results in a sizable nonzero spin current.

On the other hand, after reducing SOC ($\lambda = 0.001\lambda_{so}$), we observe a different picture: the band structure with

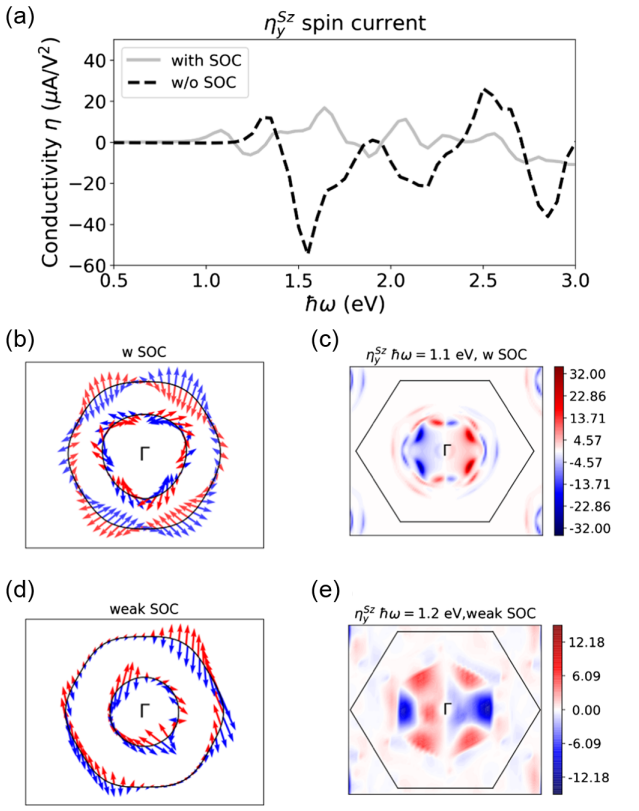

FIG. 3. (a) The y-direction photodriven spin current of the S_z component with full SOC (gray solid line) and extremely weak SOC (dashed line), i.e., SOC strength $\lambda = 0.001\lambda_{so}$. The spin texture of valence bands at $E = -0.17$ eV in Fig. 2(b) with full SOC (b) and extremely weak SOC (d). The spin photoconductivity distribution in k space with full SOC (c) and extremely weak SOC (e).

negligible SOC is symmetrical because of the SU(2) symmetry, as shown in Fig. 3(d). However, the spin texture does not exhibit any symmetry. Therefore, spin current contributed by k and $-k$ points still cannot cancel each other, resulting in a nonzero value. Figure 3(e) confirms this asymmetric spin photoconductivity distribution for photon energy at 1.2 eV.

Large photodriven spin current in 3D materials.—Since the Néel temperature of bilayer CrI_3 is around 40 K [17], we take bulk α-Fe_2O_3, i.e., hematite, as an example to demonstrate the spin photocurrent in room-temperature AFMs, in which long-distance spin transport was reported [57]. Bulk hematite is the most stable form of iron oxides, exhibiting an AFM order with the space group $R\bar{3}c$ and point group D_{3d}. The magnetic moments of adjacent Fe^{3+} layers form a AFM ordering [58]. Below the Morin temperature ($T_M \approx 263$ K), the direction of the magnetic moments is parallel to the z axis [59] as shown in Fig. 4(a). Hematite below T_M preserve the PT symmetry, where the symmetry center is labeled as a dashed circle in Fig. 4(a). Therefore, it is an excellent candidate to demonstrate photodriven spin current in weak-relativistic systems at

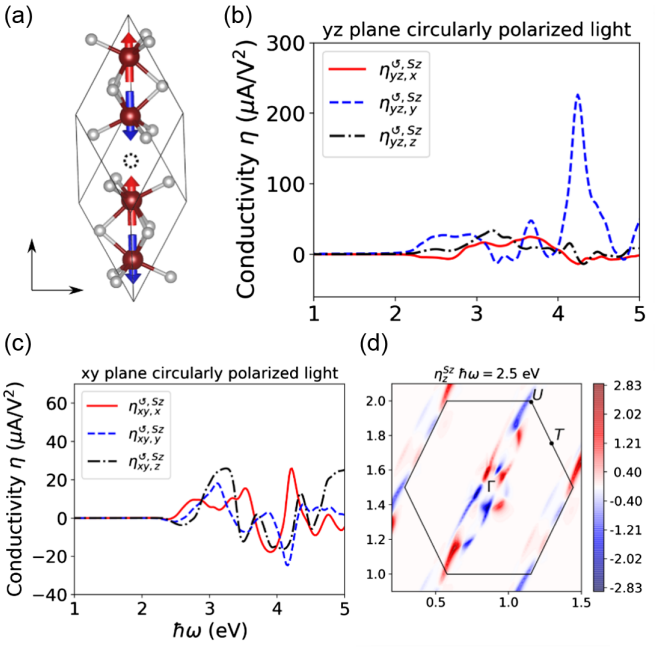

FIG. 4. (a) The atomic structure of bulk α-Fe_2O_3, the dashed circle being the PT-symmetry center. The spin S_z component photoconductivity for the polarization of circularly polarized light in yz plane (b) and in xy plane (c). The spin photoconductivity distribution in k space for ($\eta^{\circlearrowleft,Sz}_{xy,z}$) (d).

room temperature. Although spin current under linearly polarized light was predicted in hematite by considering the shift-current mechanism [31], a simultaneously excited strong charge current substantially reduces the spin polarization. In the following, we will show that circularly polarized light can overcome this problem via the proposed spin CPGE.

We have calculated the photoconductivity $\eta^{\circlearrowleft,Sz}$ according to Eq. (1) by using a conservative relaxation time, $\tau = 0.1$ ps. The magnetic group of hematite is associated with the reduction to C_3 symmetry, deriving from the representations A_{2g}. For the Sz-component spin photocurrent under circularly polarized light within the xz and yz planes, there are six nonzero tensor elements satisfying $\eta^{\circlearrowleft,Sz}_{zx,x} = \eta^{\circlearrowleft,Sz}_{yz,y}$, $\eta^{\circlearrowleft,Sz}_{zx,y} = \eta^{\circlearrowleft,Sz}_{yz,x}$, and $\eta^{\circlearrowleft,Sz}_{zx,z} = \eta^{\circlearrowleft,Sz}_{yz,z}$. We plot all nonequivalent current tensor elements, e.g., the tensor elements when the polarization of circularly polarized light is set in yz plane [Fig. 4(b)] and xy plane [Fig. 4(c)]. Interestingly, the magnitude of spin photoconductivity is in the same order or even higher than that of large SOC materials, e.g., bilayer CrI_3. For example, the magnitude of photoconductivity ($\eta^{\circlearrowleft,Sz}_{yz,y}$) can reach up to 200 $\mu A/V^2$ as shown in Fig. 4(b). Such sizable spin photoconductivity is about one order larger than that of the charge photoconductivity of $BaTiO_3$ due to BPVE [48], and the same order as that of charge photoconductivity because of CPGE in polar insulators, e.g., GeSe [39] and CdSe [52]. Figure 4(d) shows the Sz spin photoconductivity of z-direction current under an xy-plane circularly polarized light ($\eta^{\circlearrowleft,Sz}_{xy,z}$) that is distributed in the ΓTU plane of reciprocal space (see the plane in Supplemental Material [40]). Similar to the weak SOC result in Fig. 3(e) for CrI_3, we do not observe any symmetry of spin conductivity in k space, leading to a nonzero spin photocurrent.

Outlook.—We demonstrate a spin-CPGE effect for generating highly spin-polarized current in PT-symmetric AFM insulators. Such spin CPGE is accessible in traditional and emerging AFM insulators. Among them are NiO [60] and Cr_2O_3 [61], which have been used to generate magnon spin current [5], emerging 2D AFM insulators, such as the $MnPS_3$ family [8,16], and topological axion insulators, such as the even-layer $Mn_2Bi_2Te_4$ family [62,63]. Our prediction will not only be helpful to understand recent important measurements of vertical-direction photocurrent or spin photocurrent in CrI_3 junction devices [64], but also build a general framework to search for efficient spin pumping via light-matter interactions.

R. F. thanks Zhiqiang Bao for fruitful discussions. R. F. is supported by the Air Force Office of Scientific Research (AFOSR) Grant No. FA9550-20-1-0255, and L. Y. is supported by the National Science Foundation (NSF) Grant No. DMR-2124934. The computational resources are provided by the Extreme Science and Engineering Discovery Environment (XSEDE), which is supported by National Science Foundation (NSF) Grant No. ACI-1548562. The authors acknowledge the Texas Advanced Computing Center (TACC) at The University of Texas at Austin for providing HPC resources.

Note added.—Recently, we became aware of theoretical studies by Haowei Xu *et al.* [65], which show spin photocurrent of AFM $MnBi_2Te_4$.

*ruixiangfei@gmail.com
†lyang@physics.wustl.edu

[1] V. Baltz, A. Manchon, M. Tsoi, T. Moriyama, T. Ono, and Y. Tserkovnyak, Rev. Mod. Phys. **90**, 015005 (2018).
[2] T. Jungwirth, X. Marti, P. Wadley, and J. Wunderlich, Nat. Nanotechnol. **11**, 231 (2016).
[3] T. Jungwirth, J. Sinova, A. Manchon, X. Marti, J. Wunderlich, and C. Felser, Nat. Phys. **14**, 200 (2018).
[4] R. Cheng, J. Xiao, Q. Niu, and A. Brataas, Phys. Rev. Lett. **113**, 057601 (2014).
[5] J. Li, C. B. Wilson, R. Cheng, M. Lohmann, M. Kavand, W. Yuan, M. Aldosary, N. Agladze, P. Wei, M. S. Sherwin, and J. Shi, Nature (London) **578**, 70 (2020).
[6] P. Vaidya, S. A. Morley, J. van Tol, Y. Liu, R. Cheng, A. Brataas, D. Lederman, and E. del Barco, Science **368**, 160 (2020).
[7] O. Gomonay, V. Baltz, A. Brataas, and Y. Tserkovnyak, Nat. Phys. **14**, 213 (2018).
[8] R. Cheng, S. Okamoto, and D. Xiao, Phys. Rev. Lett. **117**, 217202 (2016).

[9] V. A. Zyuzin and A. A. Kovalev, Phys. Rev. Lett. **117**, 217203 (2016).
[10] S. M. Wu, W. Zhang, A. KC, P. Borisov, J. E. Pearson, J. S. Jiang, D. Lederman, A. Hoffmann, and A. Bhattacharya, Phys. Rev. Lett. **116**, 097204 (2016).
[11] S. Seki, T. Ideue, M. Kubota, Y. Kozuka, R. Takagi, M. Nakamura, Y. Kaneko, M. Kawasaki, and Y. Tokura, Phys. Rev. Lett. **115**, 266601 (2015).
[12] H. T. Simensen, A. Kamra, R. E. Troncoso, and A. Brataas, Phys. Rev. B **101**, 020403 (2020).
[13] E. Y. Sherman, A. Najmaie, H. M. van Driel, A. L. Smirl, and J. E. Sipe, Solid State Commun. **139**, 439 (2006).
[14] P. Němec, M. Fiebig, T. Kampfrath, and A. V. Kimel, Nat. Phys. **14**, 229 (2018).
[15] Z. Ni, K. Wang, Y. Zhang, O. Pozo, B. Xu, X. Han, K. Manna, J. Paglione, C. Felser, A. G. Grushin, F. de Juan, E. J. Mele, and L. Wu, Nat. Commun. **12**, 154 (2021).
[16] H. Chu, C. J. Roh, J. O. Island, C. Li, S. Lee, J. Chen, J.-G. Park, A. F. Young, J. S. Lee, and D. Hsieh, Phys. Rev. Lett. **124**, 027601 (2020).
[17] Z. Sun, Y. Yi, T. Song, G. Clark, B. Huang, Y. Shan, S. Wu, D. Huang, C. Gao, Z. Chen, M. McGuire, T. Cao, D. Xiao, W.-T. Liu, W. Yao, X. Xu, and S. Wu, Nature (London) **572**, 497 (2019).
[18] W. Kraut and R. von Baltz, Phys. Rev. B **19**, 1548 (1979).
[19] J. E. Sipe and A. I. Shkrebtii, Phys. Rev. B **61**, 5337 (2000).
[20] D. E. Parker, T. Morimoto, J. Orenstein, and J. E. Moore, Phys. Rev. B **99**, 045121 (2019).
[21] T. Morimoto and N. Nagaosa, Sci. Adv. **2**, e1501524 (2016).
[22] V. M. Fridkin, A. A. Grekov, P. V. Ionov, A. I. Rodin, E. A. Savchenko, and K. A. Mikhailina, Ferroelectrics **8**, 433 (1974).
[23] A. M. Glass, D. von der Linde, and T. J. Negran, Appl. Phys. Lett. **25**, 233 (1974).
[24] Y. Zhang, T. Holder, H. Ishizuka, F. de Juan, N. Nagaosa, C. Felser, and B. Yan, Nat. Commun. **10**, 1 (2019).
[25] R. Fei, W. Song, and L. Yang, Phys. Rev. B **102**, 035440 (2020).
[26] H. Wang and X. Qian, npj Comput. Mater. **6**, 199 (2020).
[27] H. Watanabe and Y. Yanase, Phys. Rev. X **11**, 011001 (2021).
[28] S. A. Tarasenko and E. L. Ivchenko, J. Exp. Theor. Phys. Lett. **81**, 231 (2005).
[29] E. L. Ivchenko and S. A. Tarasenko, Semicond. Sci. Technol. **23**, 114007 (2008).
[30] J. Rioux and G. Burkard, Phys. Rev. B **90**, 035210 (2014).
[31] S. M. Young, F. Zheng, and A. M. Rappe, Phys. Rev. Lett. **110**, 057201 (2013).
[32] W.-Y. Shan, J. Zhou, and D. Xiao, Phys. Rev. B **91**, 035402 (2015).
[33] S. D. Ganichev, E. L. Ivchenko, V. V. Bel'kov, S. A. Tarasenko, M. Sollinger, D. Weiss, W. Wegscheider, and W. Prettl, Nature (London) **417**, 153 (2002).
[34] S. D. Ganichev, S. A. Tarasenko, V. V. Bel'kov, P. Olbrich, W. Eder, D. R. Yakovlev, V. Kolkovsky, W. Zaleszczyk, G. Karczewski, T. Wojtowicz, and D. Weiss, Phys. Rev. Lett. **102**, 156602 (2009).
[35] P. Olbrich, C. Zoth, P. Lutz, C. Drexler, V. V. Bel'kov, Y. V. Terent'ev, S. A. Tarasenko, A. N. Semenov, S. V. Ivanov, D. R. Yakovlev, T. Wojtowicz, U. Wurstbauer, D. Schuh, and S. D. Ganichev, Phys. Rev. B **86**, 085310 (2012).
[36] R.-C. Xiao, D.-F. Shao, Y.-H. Li, and H. Jiang, npj Quantum Mater. **6**, 35 (2021).
[37] R. Fei, X. Lu, and L. Yang, arXiv:2006.10690.
[38] J. Shi, P. Zhang, D. Xiao, and Q. Niu, Phys. Rev. Lett. **96**, 076604 (2006).
[39] S. R. Panday, S. Barraza-Lopez, T. Rangel, and B. M. Fregoso, Phys. Rev. B **100**, 195305 (2019).
[40] See Supplemental Material at http://link.aps.org/supplemental/10.1103/PhysRevLett.127.207402 for the first-principles computational details, band structures, spin photocurrent spectrum, shift current under circularly polarized light, and charge photocurrent spectrum.
[41] G. Kresse and J. Furthmüller, Phys. Rev. B **54**, 11169 (1996).
[42] G. Kresse and D. Joubert, Phys. Rev. B **59**, 1758 (1999).
[43] J. P. Perdew, K. Burke, and M. Ernzerhof, Phys. Rev. Lett. **77**, 3865 (1996).
[44] B. Huang, G. Clark, D. R. Klein, D. MacNeill, E. Navarro-Moratalla, K. L. Seyler, N. Wilson, M. A. McGuire, D. H. Cobden, D. Xiao, W. Yao, P. Jarillo-Herrero, and X. Xu, Nat. Nanotechnol. **13**, 544 (2018).
[45] N. Sivadas, S. Okamoto, X. Xu, C. J. Fennie, and D. Xiao, Nano Lett. **18**, 7658 (2018).
[46] K. Kaasbjerg, K. S. Thygesen, and K. W. Jacobsen, Phys. Rev. B **85**, 115317 (2012).
[47] L. Yang, N. A. Sinitsyn, W. Chen, J. Yuan, J. Zhang, J. Lou, and S. A. Crooker, Nat. Phys. **11**, 830 (2015).
[48] S. M. Young and A. M. Rappe, Phys. Rev. Lett. **109**, 116601 (2012).
[49] X. Mu, Y. Pan, and J. Zhou, npj Comput. Mater. **7**, 61 (2021).
[50] J. Hübner, W. W. Rühle, M. Klude, D. Hommel, R. D. R. Bhat, J. E. Sipe, and H. M. van Driel, Phys. Rev. Lett. **90**, 216601 (2003).
[51] H. Zhao, X. Pan, A. L. Smirl, R. D. R. Bhat, A. Najmaie, J. E. Sipe, and H. M. van Driel, Phys. Rev. B **72**, 201302(R) (2005).
[52] N. Laman, A. I. Shkrebtii, J. E. Sipe, and H. M. van Driel, Appl. Phys. Lett. **75**, 2581 (1999).
[53] D. F. Shao, S. H. Zhang, G. Gurung, W. Yang, and E. Y. Tsymbal, Phys. Rev. Lett. **124**, 067203 (2020).
[54] J. E. Hirsch, Phys. Rev. Lett. **83**, 1834 (1999).
[55] J. Sinova, D. Culcer, Q. Niu, N. A. Sinitsyn, T. Jungwirth, and A. H. MacDonald, Phys. Rev. Lett. **92**, 126603 (2004).
[56] A. Manchon, J. Železný, I. M. Miron, T. Jungwirth, J. Sinova, A. Thiaville, K. Garello, and P. Gambardella, Rev. Mod. Phys. **91**, 035004 (2019).
[57] R. Lebrun, A. Ross, S. A. Bender, A. Qaiumzadeh, L. Baldrati, J. Cramer, A. Brataas, R. A. Duine, and M. Kläui, Nature (London) **561**, 222 (2018).
[58] L. Pauling and S. B. Hendricks, J. Am. Chem. Soc. **47**, 781 (1925).
[59] G. Rollmann, A. Rohrbach, P. Entel, and J. Hafner, Phys. Rev. B **69**, 165107 (2004).
[60] T. Kampfrath, A. Sell, G. Klatt, A. Pashkin, S. Mährlein, T. Dekorsy, M. Wolf, M. Fiebig, A. Leitenstorfer, and R. Huber, Nat. Photonics **5**, 31 (2011).
[61] S. P. Pati, M. Al-Mahdawi, S. Ye, Y. Shiokawa, T. Nozaki, and M. Sahashi, Phys. Rev. B **94**, 224417 (2016).

[62] M. M. Otrokov, I. P. Rusinov, M. Blanco-Rey, M. Hoffmann, A. Y. Vyazovskaya, S. V. Eremeev, A. Ernst, P. M. Echenique, A. Arnau, and E. V. Chulkov, Phys. Rev. Lett. **122**, 107202 (2019).

[63] C. Liu, Y. Wang, H. Li, Y. Wu, Y. Li, J. Li, K. He, Y. Xu, J. Zhang, and Y. Wang, Nat. Mater. **19**, 522 (2020).

[64] T. Song, E. Anderson, M. W.-Y. Tu, K. Seyler, T. Taniguchi, K. Watanabe, M. A. McGuire, X. Li, T. Cao, D. Xiao, W. Yao, and X. Xu, arXiv:2102.10818.

[65] H. Xu, H. Wang, J. Zhou, and J. Li, Nat. Commun. **12**, 4330 (2021).